Arab J Geosci (2017) 10:110
DOI 10.1007/s12517-017-2914-3

ORIGINAL PAPER

Groundwater occurrence and aquifer vulnerability assessment of Magodo Area, Lagos, Southwestern Nigeria

Moroof O. Oloruntola[1] · **Olateju O. Bayewu**[2] · **Ganiyu O. Mosuro**[2] · **Adetayo F. Folorunso**[3] · **Sefiu O. Ibikunle**[1]

Received: 11 May 2016 / Accepted: 14 February 2017

Abstract A combination of vertical electrical soundings (VES), 2D electrical resistivity imaging (ERI) surveys and borehole logs were conducted at Magodo, Government Reserve Area (GRA) Phase 1, Isheri, Southwestern Nigeria, with the aim of delineating the different aquifers present and assessing the groundwater safety in the area. The Schlumberger electrode array was adopted for the VES and dipole-dipole array was used for the 2D imaging. The maximum current electrode spread (AB) was 800 m and the 2D traverse range between 280 and 350 m in the east-west direction. The thickness of impermeable layer overlying the confined aquifer was used for the vulnerability ratings of the study area. Five lithological units were delineated: the topsoil, clayey sand, unconsolidated sand which is the first aquifer, a clay stratum and the sand layer that constitutes the confined aquifer horizon. The topsoil thickness varies from 0.6 to 2.6 m, while its resistivity values vary between 55.4 and 510.6 Ω/m. The clayey sand layers have resistivity values ranging from 104.2 to 143.9 Ω/m with thickness varying between 0.6 and 14.7 m. The resistivity values of the upper sandy layer range from 120.7 to 2195.2 Ω/m and thickness varies from 3.3 to 94.0 m. The resistivity of the clay layer varies from 11.3 to 96.1 Ω/m and the thickness ranges from 29.6 to 76.1 m. The resistivity value of the confined aquifer ranges between 223 and 1197.4 Ω/m. The longitudinal conductance (0.0017–0.02 mhos) assessment of the topsoil shows that the topsoil within the study area has poor overburden protective capacity, and the compacted impermeable clay layer shows that the underlying confined aquifer is well protected from contamination and can be utilized as a source of portable groundwater in the study area. This study therefore enabled the delineation of shallow aquifers, the variation of their thicknesses and presented a basis for safety assessment of groundwater potential zones in the study area.

Keywords Borehole logs · Aquifer · Resistivity · Groundwater · Protective capacity · Safety assessment

✉ Moroof O. Oloruntola
oloruntolamoroof@yahoo.com

[1] Department of Geosciences, University of Lagos, Lagos, Nigeria

[2] Olabisi Onabanjo University, Ago Iwoye, Nigeria

[3] Department of Marine Science and Technology, Federal University of Technology, Akure, Nigeria

Introduction

The geoelectrical resistivity method has been successfully employed in the delineation of subsurface geological sequence, geological structures/features of interest, aquifer units, types and depth extent in almost all geological terrains (Oladapo et al. 2004; Ako et al. 2005; Lashkaripour et al. 2005; Hassanein et al. 2007). This is because of the significant resistivity contrasts that exist between different earth materials (Olorunfemi and Fasuyi 1993). The resistivity method can therefore map interface along which a resistivity contrast exists. This interface may or may not coincide with geological boundary (Telford et al. 1990). In addition, vertical electrical sounding (VES) has been widely used to evaluate groundwater potentials and area of high groundwater yield (Ako and Osondu 1986; Abdulaziz 2005; Abiola et al. 2009). Geoelectrical methods are also used extensively in groundwater mapping for investigation of the vulnerability of shallow aquifers (Abiola et al. 2009). The vulnerability of aquifers is largely dependent on the presence or absence of protective impermeable layer, usually clay. The earth medium acts as a natural filter to percolating fluid; its ability to retard and filter

Published online: 02 March 2017

percolating fluid is a measure of its protective capacity (Olorunfemi et al. 1998). Studies such as Sørensen et al. (2005) have shown that geoelectrical method is an invaluable tool in mapping aquifer vulnerability because of its capability to distinguish low- and high-resistive formations.

Many studies (Olayinka and Olorunfemi 1992; Oladapo and Akintorinwa 2007; Olorunfemi and Fasuyi 1993) have employed electrical resistivity methods in solving problems associated with groundwater occurrences, potential and pollution in many parts of southwestern Nigeria. Most of these studies have been focused principally in areas underlain by basement complex rocks. This is largely due to the localized and irregular nature of groundwater occurrence in basement complex terrains. The few works carried out using electrical resistivity studies in sedimentary areas are mostly related to groundwater pollution problems and foundation studies. In most of the sedimentary basins in Nigeria, several aquifers have been mapped through borehole logs; hence, the only major well-known problem associated with groundwater occurrence is few areas where the aquifers occur at deep depth, raising the cost of constructing boreholes for domestic water supply.

In Lagos area, four aquifers have been mapped out from few lithologic logs, occurring at varying depths in different parts of the state (Olatunji 2006, unpublished). In recent years, inadequate municipal water supply has led to the emergence of wells/boreholes in many parts of the city, including Magodo and its environs. Many problems have been reported ranging from poor water quality (Olatunji et al. 2005) to unsuccessful wells/boreholes. Most importantly, adjoining areas having similar geology have been reported to be characterized by rapidly changing facie, presence of thick clay layer, and vulnerability of groundwater to pollution from surface sources (Ako et al. 2005). In several places such as Imota, Magodo, and some parts of Ikorodu, many failed boreholes have been reported, largely attributable to very poor borehole construction procedures. Many low-yield boreholes have been drilled within the Magodo area, and a number of failed boreholes are also common. In addition, the area is rapidly developing, population is rapidly growing and industrial/business activities are springing up, leading to uncontrolled location of facilities like septic tanks of various households which can invoke permanent pollution on the underlying aquifers. Thus, the study therefore also seeks to evaluate the protective capacity of the overburden materials in order to establish the level of safety of the groundwater resources within the estate.

This study therefore seeks to use geoelectric resistivity sounding data, 2D electrical resistivity imaging, and borehole logs information to delineate the strata boundaries, subsurface disposition, and assess the vulnerability status of the shallow water bearing aquifers in Magodo Government Reserved Area (GRA) phase 1, Isheri, Lagos, Southwestern Nigeria (Fig. 1). The study is focused on enhancing the success rate of boreholes in the area, and it also intends to characterize the aquifer.

The study area

The study area is located in Magodo GRA Phase1, Isheri, Lagos, between latitudes 6°37′667″ N and 6°38′117″ N and longitudes 3°22′906″ E and 3°22′887″ E (Fig. 1). The area is in the tropical rain forest zone of Nigeria, characterized by long wet season spanning from April to September and short dry seasons spanning from November to March (Akintola 1986). The average rainfall is between 40 and 60 mm, with peak rainfall between the months of May and August. The temperature range is between 25 and 27 °C (Odemerho and Onokerheraye 1994). Two major landform units, namely the flat topography and Ogun River Valley, dominate the study area. The flat topography is the most extensive landform system in the area, with the elevation ranging between 27 and 45 m above sea level.

The study area is located within the Dahomey Basin (Fig. 2). The stratigraphy of Cretaceous to Tertiary sedimentary sequence of the Eastern Dahomey Basin can be divided into Abeokuta Group, Imo Group, Ilaro Formation, Coastal Plain Sands, and Recent Alluvium (Omatsola and Adegoke 1981). The recent alluvium deposits, the continental Benin sands, and the Ilaro Formations were identified as the major aquifers (Longe et al. 1987). The aquifers are essentially made

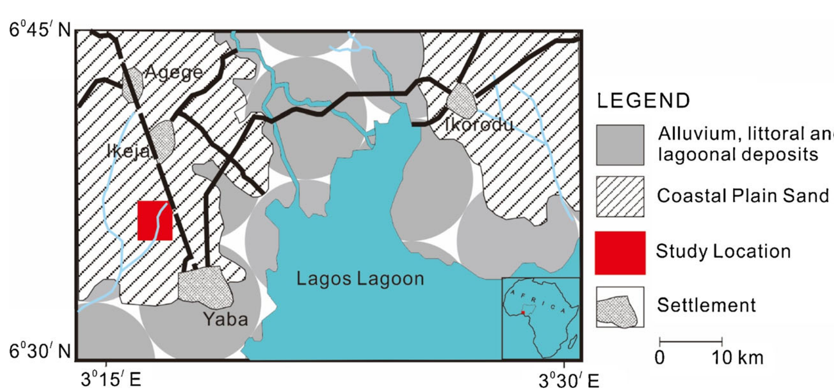

Fig. 1 The location map of the study area showing Recent Alluvium and Coastal Plain Sands

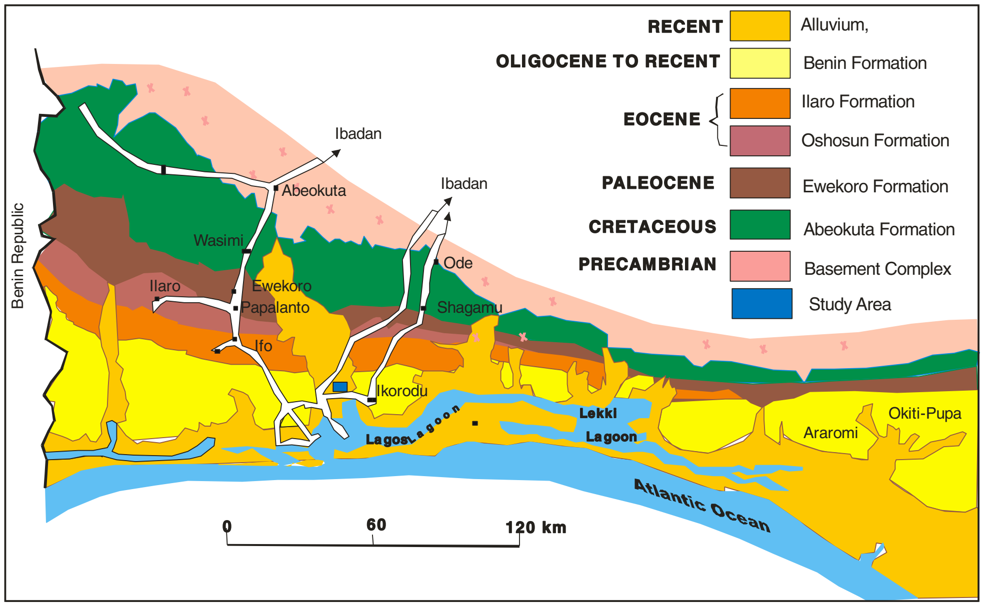

Fig. 2 Geological Map of the Nigerian part of the Dahomey Basin (modified after Gebhardt et al. 2010)

of sands, gravels, or a mixture of the two. These aquifers are generally shallower than 200 m and can be classified into three types (Longe et al. 1987). Four distinct aquifers are present in the study area. The first is a water table aquifer that is prone to pollution because of its unconfined condition. The other aquifers are confined by overlying and underlying impervious clay layers (Olatunji 2006, unpublished).

Data and methods

The vertical electrical sounding (VES) and the 2D electrical resistivity imaging were carried out at different locations shown in Fig. 3. The results of these were also compared to the data from the three borehole logs of wells drilled in the study area (Fig. 4).

Borehole logs

The three borehole logs were acquired from Terra Aqua, a borehole drilling company. Well Bh1 is a low-yielding borehole close to Traverse 1, and Bh2 is also a low-yielding well drilled in an area along Traverse 2, while Bh3 is a failed borehole within the study area.

Vertical electrical sounding

A total of thirty-three VES stations were established along the traverses using PASI Resistivity meter with maximum electrode spread (AB) of 800 m. The data acquired were processed to remove random noise such as noise due to instrumentation and the environment. The quantitative interpretation of the depth sounding curves was carried out through the partial curve matching technique (Bhattacharya and Patra 1968), where the plotted VES data were matched on the standard two (2) layer master curve and four (4) auxiliary type curves (H, K, A, and Q). The layer models from the partial curve marching were then used to constrain the interpretation by the computer using iteration software known as WINRESIST in order to reduce overestimation of depths.

2D resistivity imaging

The 2D–electrical resistivity imaging traverses was done using the dipole-dipole configuration. The length of the 2D electrode traverse was 280 m along NW-SE direction. The data acquired were processed using RES2DINV program. The program basically determines a resistivity model that approximates the measured data within the limits of data errors and which is in agreement with all prior information. The difference between the measured and calculated apparent resistivity values is given by the root-mean-square (RMS) error. The data was processed to the lowest allowable root-mean-square (RMS) error.

Estimation of aquifer protective capacity

The estimation of the aquifer protective capacity was based on the values of the longitudinal unit conductance of the overburden rock units using the longitudinal conductance/protective capacity rating as indicated by Oladapo and Akintorinwa (2007).

The total transverse resistance R is given by:

$$R = \sum_{i=1}^{n} \text{hipi} \quad (1)$$

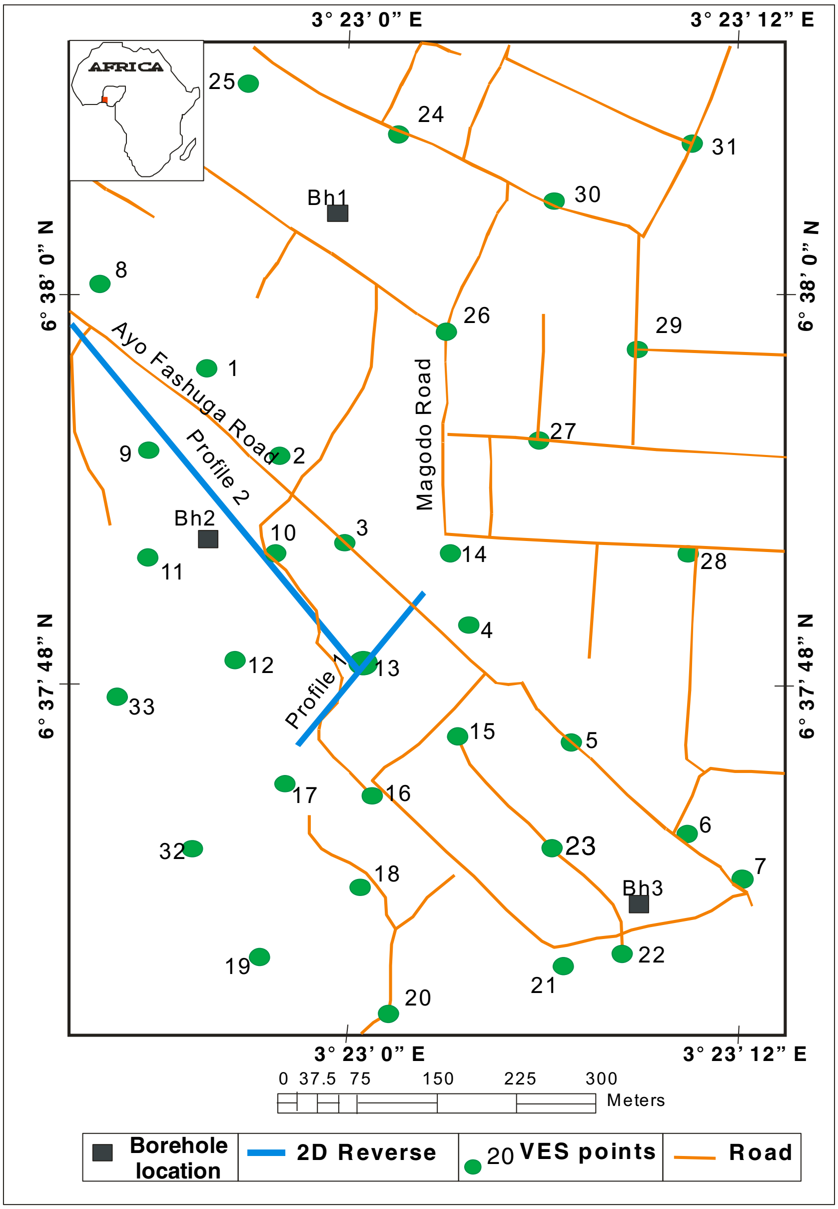

Fig. 3 Map of the Study Area showing the VES points, 2D traverses and Borehole locations within the Coastal Plain Sands

For a horizontal, homogeneous, and isotropic medium

$$\rho = \frac{(R_1 - R_2)}{(h_1 - h_2)} \qquad (2)$$

where h_i and ρ_i are the thickness and resistivity of the ith layer in the section, respectively.

The total longitudinal conductance S is:

$$S = \sum_{i=1}^{n} \frac{hi}{\rho i} \qquad (3)$$

The longitudinal layer conductance Si can also be expressed by

$$\mathrm{Si} = \sigma \mathrm{i}\, h_i \qquad (4)$$

where h_i is the layer thickness and ρ_i is layer resistivity, while the number of layers from the surface to the top of aquifer varies from $i = 1$ to n.

The longitudinal layer conductance (S) of the overburden at each VES station was obtained from first-order resistivity data using Eq. 3 (Reynolds 1997). To obtain a layer parameter, a unit square cross-sectional area is cut out of a group of n-layers of infinite lateral extent.

The modified longitudinal conductance/protective capacity rating as shown in Table 1 was used as a guide for the classification of the protective capacity rating. The longitudinal conductance maps were generated using surfer software. The topsoil longitudinal conductance values were obtained from Eq. 1.

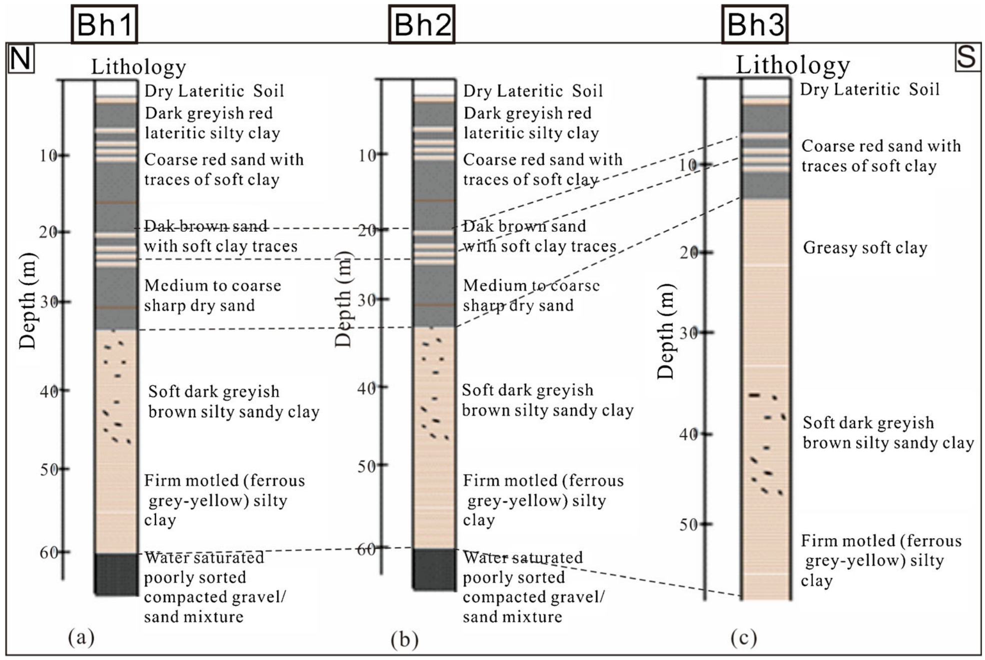

Fig. 4 Borehole log penetrating the Coastal Plain sands of well (Bh1), a low yielding well close to section A-A′ (*a*), well (Bh2) a low yielding well close to section D-D ′ of the study area (b), and well (Bh3), a failed borehole around section C-C′ of the study area (*c*)

Results and discussions

The results showing the various geoelectric layers delineated and corresponding inferred lithology were presented as geoelectric sections, isoresistivity, and depth to the top of the aquifer zone maps.

The curve types (Fig. 5) which reflect the lithological variations in the study area include AKH (33%), AK (27%), KH (12%), and AKQ, HKH, HK, and QH accounts for about 6%. The general signature of the curves suggests alternate sequence of resistive-conductive layers, reflecting the lithology of the coastal plain sequence, characterized by intercalation of sands and clay horizons as described by Omosuyi et al. (1999). The curves reflect the alternating sequence of clay (low resistivity), and sands are shown Fig. 4.

Geoelectric section

The geoelectric section along Traverse 1 revealed four to five geoelectric layers (Fig. 6). The topsoil varies in lithology from clay through clayey sands to sands along the traverse having resistivity values of between 58.7 and 229.5 Ωm. The second horizon is essentially sandy having resistivity values of 263.0 to 1223.2 Ωm. This layer constitutes the upper aquifer with thickness of 21.8 to 78.1 m. The third horizon consists of clay layer (Fig. 4), having thickness of up to 41.4 m. The resistivity value of this layer ranges between 36 and 117.1 Ωm reflecting variation of the clay across the area. This thick clay stratum serves as a confining layer for the aquifers above and below it, hence making the aquifers confined and protecting the layer from contamination. The last geoelectrical layer is composed of sand that constitutes the confined aquifer at some of the locations. The resistivity varies from 675.0 to 1650.0 Ωm; although poorly sorted, it consists of fine to medium grains sand, but the sandy layer is saturated as confirmed from the well (Bh2) around the traverse.

Table 1 Modified longitudinal conductance/protective capacity rating (Oladapo and Akintorinwa 2007)

Longitudinal conductance (mhos)	Protective capacity rating
>10	Excellent
5–10	Very good
0.8–4.9	Good
0.2–0.79	Moderate
0.1–0.19	Weak
<0.1	Poor

Traverse 3 (Fig. 7) covering other parts of the study area indicates similar trends. Based on the resistivity values, the topsoil grades from clay to sands across the study area (Fig. 7). Underlying the topsoil is essentially sandy horizon with variation in coarseness and sorting of the sands across the study area. This is supported by the variation in resistivity values and cuttings from the boreholes. The third continuous horizon is composed largely of clay (Fig. 4) separating the sands above from the sand below. The thickness of the clay layer varies across the area from 23.8 to 120.7 Ω/m, with thickness of between 41.4 and 83.0 m in area where the thickness could be determined. The lower sand (i.e., second aquifer) is found at depth ranging from 40 to 70 m beneath the impervious clay.

Fig. 5 The dominants VES curve types in the study area

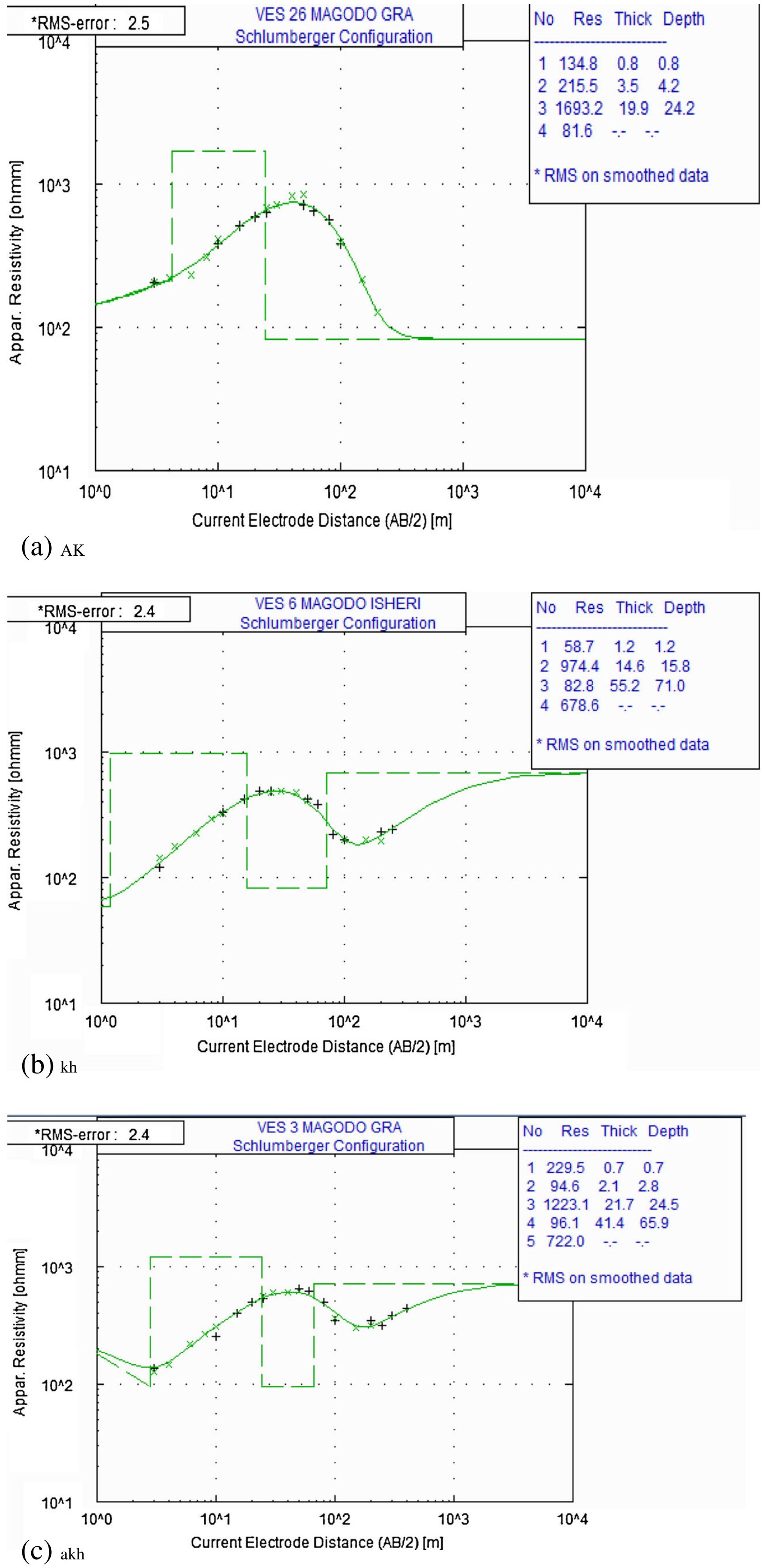

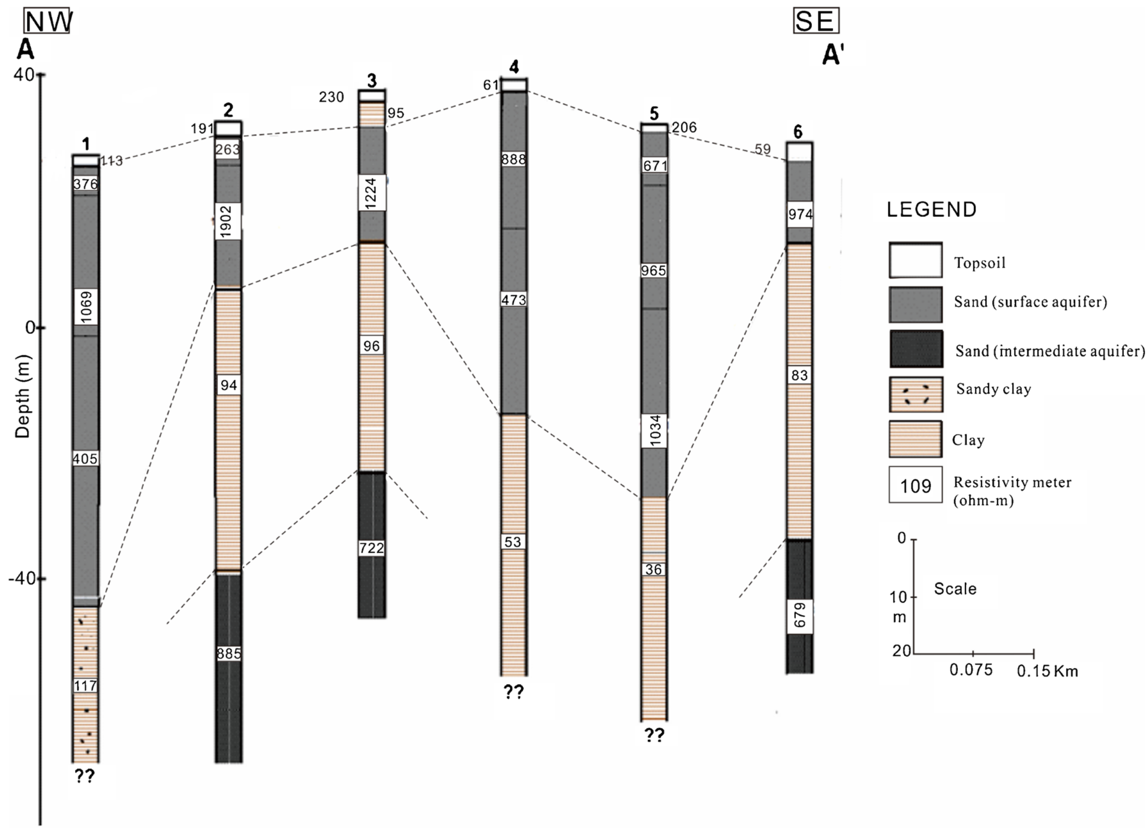

Fig. 6 The geoelectric section along Traverse 1 in the study area (NW-SE Direction), showing succession of sandy and clayey horizons within the Coastal Plain Sands

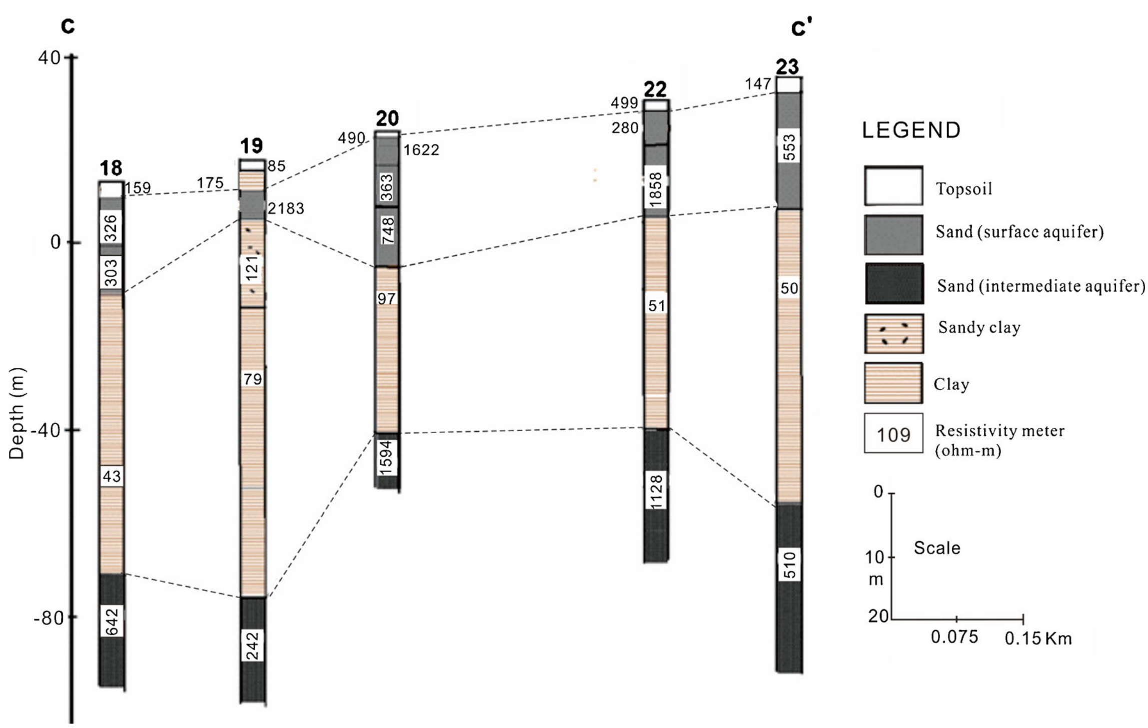

Fig. 7 Geo-electric Section along Traverse 3 in the study area (North-South Direction), showing succession of sandy and clayey horizons within the Coastal Plain Sands

Isoresistivity maps

Porosity and permeability are important hydrogeologic parameters often synonymous with groundwater saturation (Okosun 1998). Omosuyi (2001) has shown that the sands of the Coastal Plain are usually characterized by high resistivity, deriving from the coarse, gravely nature, rather than a measure of groundwater saturation disposition. Thus, the isoresistivity maps showing resistivity variation within the delineated horizon were generated for the upper aquifers (Fig. 8). The overall assessment of the upper aquifer indicates that the materials that make up this aquiferous layer (Fig. 8a) have relatively high resistivity values varying from approximately 121 to 2195 Ωm and a mean value of ca. 664 Ωm. As observed from the borehole cuttings, this layer indicates lithology characterized by unconsolidated poorly sorted gravels and medium to coarse-grained sands, intercalated with fine-grained sands, sometimes with little silts and clay. The unconsolidated nature of the coarse-grained sand/gravel is inferred from Bh1, Bh2, and Bh3 (Fig. 4). The coarseness gives the aquifer more potential to store and transmit groundwater, as the porosity and permeability of an aquifer depends on the grain size distribution.

Map of the clay layer overlying the confined aquifer

Kalinski et al. (1993) have shown that the thickness and resistivity parameters of materials overlying an aquifer are important parameters in the assessment of the vulnerability of the underling aquifer. The isopach map of the depth to aquifer depicts the variation in the thickness of aquifer overburden. The thickness distribution of the clay formation varies from 30 to 76 m (Fig. 9). The thickness of the clay layer increases in the southwestern direction. From less than 15 m around the NE, and between 15 and 30 m in most part of the study area and greater than 30 m in a few areas, this variation in thickness of the overlying clay stratum is a major factor that influences the variation of depth to the lower aquifer delineated in the study area.

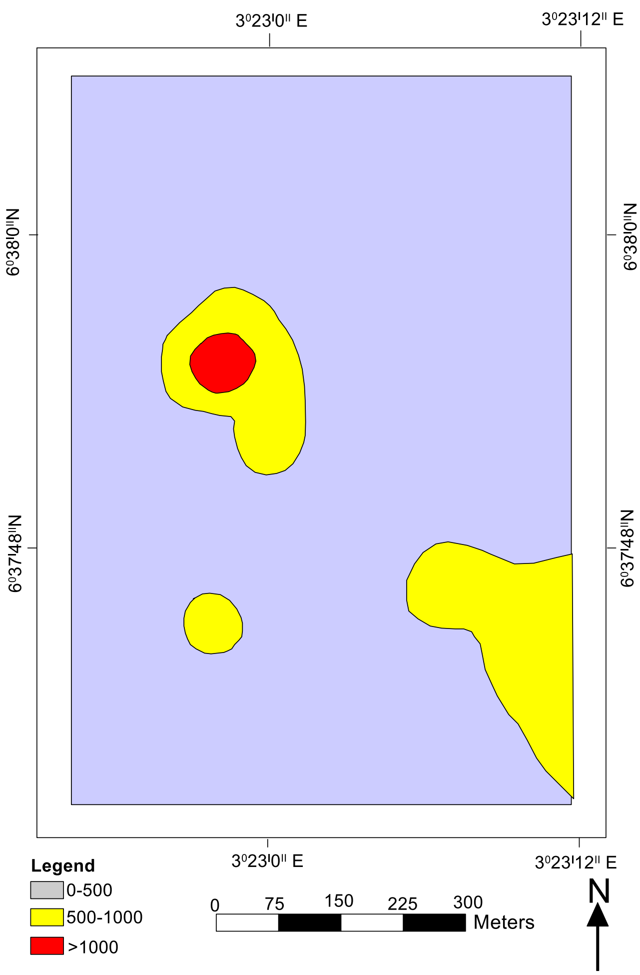

Fig. 8 Isoresistivity map of the upper aquifer, a sandy layer within the Coastal Plain sands

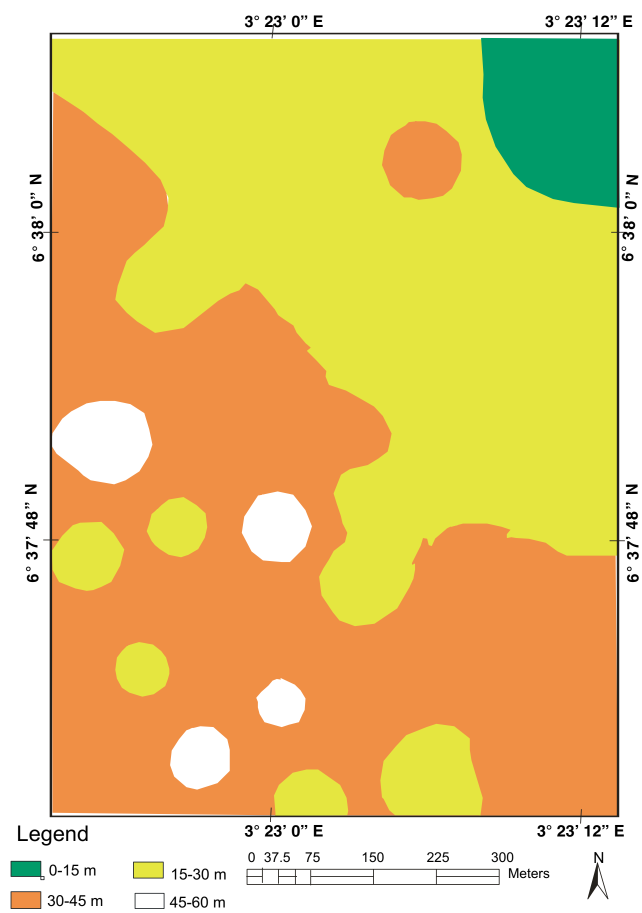

Fig. 9 Isopach Map of the Clay layer within the Coastal Plain sands in the study area

Aquifer potential and vulnerability potential rating and protective capacity rating

Kelly (1976) and Mbonu et al. (1991) have shown that areas with thick aquifer unit may be good prospects for drilling boreholes with high yield expectations. The assessment of the potentials of the surface and the confined aquifer units in this study presented in Table 2 was based on the aquifer thickness derived from VES data interpretation and overburden thickness. The area has been grouped into three based on aquifer thickness as follows: good with thickness value (>30 m), fair (15–30 m), and poor for values (<15 m) groundwater prospect zones. The vulnerability rating was also grouped into three categories based on overburden thickness, with value less than 1.0 m classified as poor, 1.0–5.0 m as weak, and greater than 5.0 m as excellent.

The overall vulnerability to contamination of this aquifer in these regions is high. This among other environmental factors can lead to serious environmental hazards if not considered and prevented early enough.

Table 2 A summary of the nature and potential rating of the aquifer units

VES	Nature Of aquifer	Thickness	Potential rating	Clay thickness	Depth to the top of aquifer	Vulnerability rating
1	Confined	79.8	Medium	Undetermined	3.6	Weak
2	Unconfined	18.2	Low	49.9	4.4	Weak
	Confined				72.5	Excellent
3	Unconfined	21.7	Medium	41.4	0.9	Poor
	Confined				65.9	Excellent
4	Confined	56.2	Medium	29.6	0.9	Poor
5	Unconfined	65.1	Medium	Undetermined	0.6	Poor
6	Confined	14.6	Low	55.2	1.2	Weak
					71	Excellent
7	Unconfined	10.1	Low	36.2	16.1	Excellent
	Confined				49.6	Excellent
8	Unconfined	19.8	Medium	57.4	5.8	Excellent
	Confined				93.4	Excellent
9	Confined	77.8	Medium	52	4.1	Weak
					82.5	Excellent
10	Confined	17.5	Medium	47	13.3	Excellent
					77.8	Excellent
11	Confined	21.7	Low	73.4	1.2	Weak
					95.2	Excellent
12	Unconfined	3.3	Medium	76.1	1	Weak
13	Confined	28.2	Medium	Undetermined	5.8	Excellent
14	Unconfined	94	High	43.1	0.9	Poor
15	Confined	85.2	High	–	1.4	Weak
16	Unconfined	27.2	Medium	52.3	6.2	Excellent
	Confined				79.5	Excellent
17	Unconfined	1	Medium	50.8	2	Weak
	Confined				76.5	Excellent
18	Unconfined	23.7	Medium	61.1	1.2	Weak
	Confined				86.8	Excellent
19	Confined	3.9	Medium	62.8	0.5	Poor
					89.1	Excellent
20	Unconfined	18	Low	32	0.7	Poor
	Confined				50.5	Excellent
21	Confined	58.3	High	–	0.5	Poor
22	Unconfined	14.8	Medium	44.9	0.9	Poor
	Confined				66.4	Excellent
23	Unconfined	27.3	Medium	58.8	2.2	Weak
	Confined				88.3	Excellent
24	Confined	83.2	High	6	6.9	Excellent
25	Confined	80	High	Undetermined	2.6	Weak
26	Unconfined	23.4	Medium	Undetermined	0.8	Poor
27	Unconfined	25.4	Low	Undetermined	2.8	Weak
28	Confined	54.4	High	Undetermined	0.6	Poor
29	Confined	69.3	High	Undetermined	0.6	Poor
30	Confined			Undetermined	1.3	Weak
31		61.7	High	44.9	0.7	Poor
32	Confined	36.7	Medium	50.1	2.6	Weak
					89.4	Excellent
33	Confined	12.8	Low	Undetermined	0.8	Poor

Table 3 Modified longitudinal conductance/protective capacity rating

Longitudinal conductance (mhos)	Protective capacity rating
>10	Excellent
5–10	Very good
0.8–4.9	Good
0.2–0.79	Moderate
0.1–0.19	Weak
<0.1	Poor

From Oladapo and Akintorinwa (2007)

The thickness and resistivity parameters of materials overlying an aquifer are important in the assessment of the vulnerability of the underlying aquifer (Kalinski et al. 1993). The vulnerability potential rating and estimation of the aquifer protective capacity were based on the values of the longitudinal unit conductance of the topsoil at each VES station with reference to the classification of Oladapo and Akintorinwa (2007) in Table 3. The longitudinal conductance of topsoil was used because burial of utilities and underground septic tanks, which are important sources of groundwater pollution, are restricted to shallow depths. The total overburden longitudinal conductance was also used for evaluating the overburden protective capacity of the study area.

The topsoil longitudinal conductance values vary from 0.0017 to 0.02 mhos (Table 4). This shows that the topsoil within the study area has poor overburden protective capacity. As found from the borehole logs, the topsoil is largely lateritic

Table 4 Topsoil longitudinal conductance values of each VES station

VES	Thickness (m)	Resistivity (Ωm)	Overburden conductance $S = hts/\rho ts$	Protective capacity rating
1	0.6	113.2	0.005	Poor
2	1.1	190.5	0.006	Poor
3	0.7	229.5	0.003	Poor
4	0.9	61.1	0.015	Poor
5	0.6	205.6	0.003	Poor
6	1.2	58.7	0.020	Poor
7	0.8	175.5	0.005	Poor
8	0.6	97.9	0.006	Poor
9	0.8	109.7	0.007	Poor
10	1	93.5	0.011	Poor
11	1.2	89.9	0.013	Poor
12	1	222.5	0.004	Poor
13	0.7	343.7	0.002	Poor
14	0.9	505.8	0.002	Poor
15	1.2	55.4	0.022	Poor
16	0.5	176.7	0.003	Poor
17	0.6	510.6	0.001	Poor
18	2	159.2	0.013	Poor
19	0.7	84.8	0.008	Poor
20	0.5	490	0.001	Poor
21	0.9	99.2	0.009	Poor
22	0.9	498.7	0.002	Poor
23	2.2	147.4	0.015	Poor
24	0.9	255.1	0.004	Poor
25	2.6	76.5	0.034	Poor
26	0.8	134.8	0.006	Poor
27	2.8	90.9	0.031	Poor
28	0.8	43	0.019	Poor
29	0.6	138.6	0.004	Poor
30	1.3	56.8	0.023	Poor
31	0.7	118.2	0.006	Poor
32	2.6	118.2	0.022	Poor
33	0.8	66.2	0.012	Poor

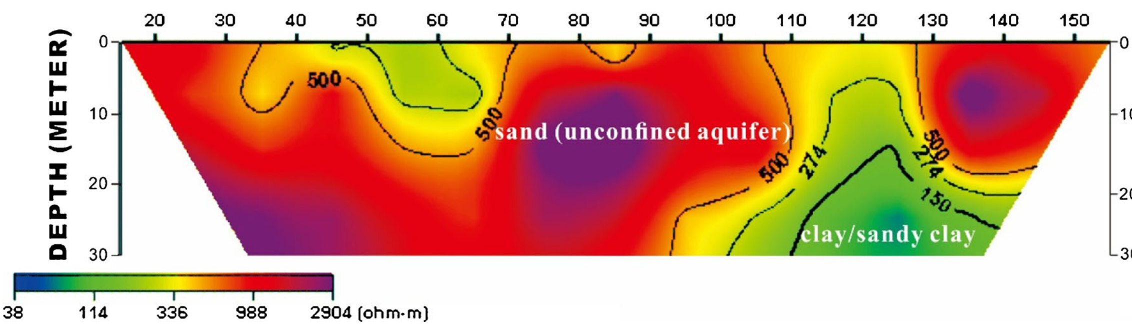

Fig. 10 The 2D inverted resistivity for profile 1

and mostly sandy in the study area. Sandy soils have a larger pore space which enables easy passage of water; hence, they are vulnerable compared to clay and shale (Chukwuma et al. 2015). The very low value of longitudinal conductance, with all the values <0.1 mhos reflecting the sandy nature of the top layer, indicates very high vulnerability of the aquifer to pollution from surface sources, especially from the nearby River Ogun. In addition, the groundwater in this estate is also vulnerable to pollution from leakages from buried underground contaminants, such as septic tanks. However, the relatively high resistivity value of the sand layer affected the estimated values.

2D electrical resistivity imaging survey

The two-dimensional (2D) inverted resistivity dipole-dipole sections on profile 1 and profile 2 shows resistivity depth models of 31 and 60 m, respectively (Figs. 10 and 11). On profile 1, resistivity model reflects the heterogeneous nature of the subsurface horizons. A good correlation exists between the borehole log of well Bh2 located around the profile and the 2D inverted model. The top layer is sandy sediment, the resistivity varies from ~300 to 600 Ωm at a depth of ~0 to >30 m from west to east end of the profile (Fig. 10). This layer is underlain by relatively high resistive sand. Beneath this layer is a continuous layer of porous and permeable layer with higher resistivity range of between 600 and 1000 Ωm, reflecting the relatively compacted nature of the aquifer with depth. The reduction in resistivity toward the eastern direction at depth below 20 m shows the rapid change in facie common in this environment as observed by Ako et al. (2005) in adjoining area to the study area. This rapid change in lithological properties common in this type of environment as reported by Ako et al. (2005) is largely responsible for the observed failure of some of the boreholes which though drilled into this same layers but hydraulic properties of the layer varies in different direction due to the abrupt change in texture of the aquiferous horizon.

Profile 2 trends in the north-west direction; the top layer revealed the presence of sandy materials, having resistivity value of 200–300 Ωm (Fig. 11). The top soil though lateritic as revealed by borehole logs is largely porous and permeable. This layer is in hydraulic continuity with sandy horizon beneath which extends from the center to the flanks of the profile up to a depth of about 40 m, having resistivity of between 200 and 500 Ωm. Saturated zone delineated using the borehole logs as control has resistivity values of 150–224 Ωm visible at a depth of 30–35 m and extends laterally across the profile. This is the unconfined aquifer delineated from the geoelectric sections. Between the lateral distance of 100 and 200 m (Fig. 11) is a low resistivity zone with a resistivity value of <100 Ωm at 40-m depth that is separated and overlain by the unconfined aquifer. The profile terminated within the clayey layer that separates the unconfined aquifer from the confined aquifer. The geoelectric sections around these profiles provide unambiguous agreement with the 2D.

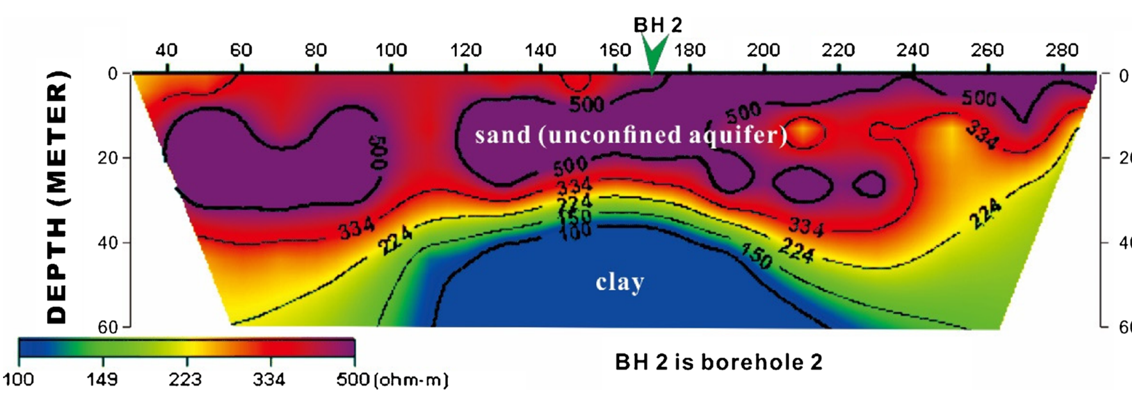

Fig. 11 The 2D inverted resistivity for profile 2 with position of Bh2 along the profile

The sandy nature of the overburden which as reported by several authors to be characterized by relatively low longitudinal conductance that offers very little protection to the underlying aquifer (Golam et al. 2014; Anomohanran 2013; Rădulescu et al. 2006). Since the unconfined aquifer within the study area is susceptible to pollution, preventive measures should be taken to protect the aquifer from degradation and ensure groundwater development for quality and sustainable water supply through instrumental approach, community participation, and adaptive measures (Ekpo et al. 2016). Although the 2D electrical resistivity imaging does not clearly reveal the presence of contamination as demonstrated by Mosuro et al. (2016), the longitudinal conductance reveals that the upper aquifer is vulnerable to pollution due to low protective capacity of the topsoil.

Conclusion

The major conclusions from the study include:

- The study area is characterized by five geoelectric layers. These layers are the top soil, clayey sand, upper sandy layer, clay, and lower sandy layer. Where sands are in hydraulic continuity to the ground surface, they are classified as unconfined, separated by clay stratum from the lower sands classified as confined aquifer.
- Areas with relatively thick sand materials (>30 m) have been identified as having the highest potentials for groundwater. Whereas areas with thickness range of 15 to 30 m are delineated as having medium potentials for groundwater, while areas with thickness less than 15 m have been delineated as low groundwater potential zones.
- The resistivity values of the upper aquifer across the study area are high, and these represent the poorly sorted and unconsolidated gravel/sand materials. The average resistivity value of the lower aquifer is higher than that of the upper aquifer, largely due to the presence of compacted poorly sorted gravelly sand.
- The sandy nature of the overburden, characterized by relatively low longitudinal conductance, offers very little protection to the underlying aquifer
- The productive probable groundwater potential zones of the upper aquifer unit are identified at the northeastern and as subordinately at the south eastern part of the study area.
- The longitudinal conductance assessment of the topsoil shows that the topsoil within the study area has poor overburden protective capacity. On the other hand, the relatively thick impermeable clay layer shows that the lower aquifer (sands) is well protected from contamination and can be utilized as a source of potable groundwater supply in the study area.

References

Abdulaziz MA (2005) Resistivity methods for groundwater exploration in the cretaceous-tertiary sedimentary sequence, east of Jeddah, Saudi Arabia. J Environ Hydrol 13(19):1–11

Abiola O, Enikanselu PA, Oladapo MI (2009) Groundwater potential and aquifer protective capacity of overburden units in ado-Ekiti, southwestern Nigeria. International Journal of Physical Sciences 4(3): 120–132

Akintola JO (1986) Rainfall distribution in Nigeria 1982–1983. Impact Publishers Nigeria Limited, Ibadan, p 371

Ako BD, Osondu VC (1986) Electrical resistivity of the Kerri-Kerri Formation, Darazo, Nigeria. J Afr Earth Sci 5(5):527–534

Ako BD, Ajayi TR, Arubayi JB, Enu EI (2005) The groundwater and its occurrence in the coastal plains sands and alluvial deposits of parts of Lagos State. Nigeria Water Resources 16:7–17

Anomohanran O (2013) Geoelectrical investigation of groundwater condition in Oleh, Nigeria. www.arpapress.com. IJRRAS 15(1): 1–5

Bhattacharya APK, Patra HP (1968) Direct current geoelectric sounding: principles and interpretations. Methods of Geochemistry and Geophysics 9(1):133

Chukwuma EC, Orakwe LC, Anizoba DC, Amaefule DO, Odoh CC, Nzediegwu C (2015) Geoelectric groundwater vulnerability assessment of overburden aquifers at Awka in Anambra State, South Eastern Nigeria. European journal of Biotechnology and Bioscience 3(1):29–34

Ekpo AE, Orakwe LC, Ekpo FE, Eyeneka FD (2016) Evaluating the protective capacity of aquifers at Uyo in Akwa Ibom state, southern Nigeria, using the vertical electrical sounding (VES) technique. IARJSET 3(1):34–39

Gebhardt H, Adekeye OA, Akande SO (2010) Late Paleocene to initial Eocene thermal maximum foraminiferabiostratigarphy and paleoecology of the Dahomey Basin, southwestern Nigeria. Gjahrbuch Der GeologischemBundesantalt. 150:407–419

Golam SS, Keramat M, Shahid M (2014) Deciphering transmissivity and hydraulic conductivity of the aquifer by vertical electrical sounding (VES) experiments in Northwest Bangladesh. Appl Water Sci

Hassanein H, El-Kaliouby H, Al-Garni MA (2007) The use of DC-resistivity to outline the subsurface hydrogeological and structural setting beneath a proposed site for subsurface DAM building, Makkah Al-Mukarramah, Saudi Arabia. Journal of King Abdul Aziz University: Earth Sciences 18(1):117–138

Kalinski RJ, Kelly WE, Bogard S (1993) Combined use of geoelectrical sounding and profiling to quantify aquifer protection properties. Groundwater. 31:538–544

Kelly EW (1976) Geoelctric sounding for delineating groundwater contamination. Groundwater 14:6–11

Lashkaripour GR, Sadeghi H, Qushaeei M (2005) Vertical electrical soundings for groundwater assessment in Southeastern Iran: a case study, J. Applied Geophy 5(1):973–977

Longe EO, Malomo S, Oloruniwo MA (1987) Hydrogeology of Lagos Metropolis. J Afr 6(2):163–174

Mbonu PD, Ebeneiro JO, Ofoegbu CO (1991) Geoelectric sounding for the determination of aquifer characteristics in parts of Umuahia area of Nigeria. SEG Geophysics 36(2):284–291

Mosuro GO, Omosanya KO, Bayewu OO, Oloruntola MO, Laniyan TA, Atobi O, Okubena M, Popoola E (2016) Assessment of groundwater vulnerability to leachate infiltration using electrical resistivity method. Appl Water Sci Springer

Odemerho FO, Onokerheraye AG (1994) Physical geography (handbook for the tropics). The Benin Social science series of Africa, University of Benin, Benin City Nigeria, 16–28, 70–71, 240–255

Okosun EA (1998) Review of the early tertiary stratigraphy of southwestern Nigeria. J of Mining and Geology 34:27–35

Oladapo MI, Akintorinwa OJ (2007) Hydrogeophysical study of Ogbese Southwestern, Nigeria. Global J Pure and Applied Sci 13(1):55–61
Oladapo MI, Muhammed NZ, Adeoye OO, Adetola BA (2004) Geoelectrical investigation of the Ondo state housing corporation estate, Ijapo, Akure, southwestern Nigeria. Journal of Mining Geology 20:412–480
Olatunji AS, Abimbola AF, Oloruntola MO, Odewande AA (2005) Hydrogeochemical evaluation of groundwater resources in shallow coastal aquifers around Ikorodu area, southwestern Nigeria. Water Resource 16:65–71
Olayinka AI, Olorunfemi MO (1992) Determination of geoelectric characteristics of Okene area and implication for boreholes siting. J Min Geol 28:403–412
Olorunfemi MO, Fasuyi SA (1993) Aquifer types, geoelectric and hydrogeologic characteristics of part of the Central Basement Terrain of Niger State Nigeria. J Afr Earth Sci 16(1):309–317
Olorunfemi MO, Ojo JS, Oladapo MI (1998) Geological hydrogeological and geophysical investigations of exposed 20″ Escravos Lagos Pipeline Technical Report
Omatsola ME and Adegoke OS (1981) Tectonic evolution and cretaceous stratigraphy of the Dahomey Basin. J Min Geol. p 130–137
Omosuyi GO, (2001). "Geophysical and Hydrogeological Investigations of Ground water Prospects in the Southern part of Ondo State, Nigeria". Ph.D. Thesis, Department of Applied Geophysics, Federal University of Technology, Akure, Nigeria. 195
Omosuyi GO, Ojo JS, Olorunfemi MO (1999) Borehole lithologic correlation and aquifer delineation in parts of the Coastal Basin of SW Nigeria. J Appl Sci 2:617–626
Rădulescu V, Rădulescu F, Stan L (2006) Geoelectrical measurements applied to the assessment of groundwater quality. GEO-ECO-MARINA
Reynolds JM (1997) An introduction to applied and environmental geophysics. Wiley, Chichester, p 778
Sørensen KI, Auken E, Christensen NB, Pellerin L (2005) An integrated approach for hydrogeophysical investigations: new technologies and a case history. In: Butler DK (ed) Near-Surface Geophysics 2, Investigations in Geophysics, 13. Society of Exploration Geophysics, 585–603
Telford WM, Geldart LP, Sheriff RE (1990) Applied geophysics. Cambridge University Press, Cambridge, p 770